Peer-reviewed version available at *Micromachines* **2020**, *11*, 514; doi:10.3390/mi11050514

Article

Label-free, high-throughput assay of human dendritic cells from whole-blood samples with microfluidic inertial separation suitable for resource-limited manufacturing

Caffiyar Mohd Yousuff[1], Kue Peng Lim[2], Ismail Hussain[1], Nor Hisham Hamid[1], Sok Ching Cheong[2] and Eric Tatt Wei Ho[1,*]

[1] Department of Electrical & Electronics Engineering, Universiti Teknologi PETRONAS, Perak, Malaysia
[2] Cancer Research Malaysia, Selangor, Malaysia
* Correspondence: hotattwei@utp.edu.my; Tel.: +6 05 368 7899

Abstract: Microfluidics technology has not impacted the delivery and accessibility of point of care health services like diagnosing infectious disease, monitoring health or delivering interventions. Most microfluidics prototypes in academic research are not easy to scale-up with industrial scale fabrication techniques and cannot be operated without complex manipulations of supporting equipment and additives such as labels or reagents. We propose a label- and reagent-free inertial spiral microfluidic device to separate red blood, white blood and dendritic cells from blood fluid for applications in health monitoring and immunotherapy. We demonstrate that using larger channel widths in the range of 200 to 600 μm allows separation of cells into multiple focused streams according to different size ranges and we utilize a novel technique to collect the closely separated focused cell streams without constricting the channel. Our contribution is a method to adapt spiral inertial microfluidic designs to separate more than two cell types in the same device which is robust against clogging, simple to operate and suitable for fabrication and deployment in resource-limited populations. When tested on actual human blood cells, 77% of dendritic cells were separated and 80% of cells remained viable after our assay.

Keywords: inertial spiral microfluidics; dendritic cell separation; resource-limited microfluidics

1. Introduction

Throughout the 30-year development history of microfluidics technologies [1], a broad array of inventive concepts, novel physics and prototype devices have been demonstrated which miniaturize fluidic manipulation to achieve large-scale, simultaneous assays with nanoliter reactions and precise manipulation and inspection of microscopic objects [2]. While microfluidics technology has emerged as a powerful laboratory tool for academic research, there is an absence of its mass adoption towards solving compelling commercial or communal problems. In healthcare, microfluidics technology has a pressing opportunity to enable point-of-care (POC) testing of infectious diseases, thereby improving health care services and patient outcomes especially in settings with limited health services or laboratory infrastructure. Microfluidics POC devices may also enable novel ways to monitor population health and improve accessibility to medical interventions delivered into bodily fluids. Cell assays which count the number of circulating white blood cells could identify when a person is fighting an infection or inflammation, possibly before symptoms manifest. Microfluidic lab-on-chips could stimulate immune cells for immunotherapy[3] which is an emerging treatment for cancer tumors.

For microfluidic devices to be widely adopted in resource-limited communities, the World Health Organisation (WHO) recommends that devices fulfill the ASSURED criteria, to be Affordable, Sensitive, Specific, User-friendly, Rapid and Robust, Equipment-free and Delivered to the people

Peer-reviewed version available at Micromachines 2020, 11, 514; doi:10.3390/mi11050514

who need it [4]. Microfluidics technology was developed to miniaturize lab-scale processes and reactions into small, portable devices for rapid processing of small fluid volumes amenable for POC operation [5]. Most inventions were focused on advancing miniaturization or improving precision control over physical forces [6]. However, innovations to improve affordability, robustness and ease of use have been neglected and microfluidic devices depend on elaborate laboratory setups. Prototypes are incompatible with industrial scale fabrication [1] nor easy to operate by untrained personnel and therefore, not accessible to resource-limited populations. Paper microfluidics [7–9] is the only major innovation in recent years to address the need for affordable and simple microfluidic devices to deliver POC health services in the developing world.

In this paper, we develop an alternative approach using inertial microfluidics to separate immune cells from blood and to select dendritic cells. There are several distinct types of white blood cells which trigger or mount innate or adaptive immune responses in the body. Cell assays that uniquely quantify the distinct white blood cell populations can yield insights into the state of an individual's immune system and health. Dendritic cells are rare immune cells that react towards foreign antigens to trigger the adaptive immune response [10]. We are especially interested to isolate dendritic cells because these cells may be stimulated with tumor-associated antigens to initiate CD8+ T lymphocytes (CD8-T) assault on tumors as an immunotherapy called dendritic cell vaccination (DCV) [11,12]. For interventions like DCV where cells must be returned to the human body, microfluidic cell assays must operate on reagent and label-free principles. Excluding the use of reagents and labels also significantly improves the affordability and ease of operating devices at the POC since it obviates the logistics of purchasing, transporting, qualifying and measuring accurate volumes of chemicals, antibodies or beads.

Microfluidic devices utilizing inertial forces are capable of high-throughput, label- and reagent-free cell selection [13–17]. Inertial microfluidics utilize the shape of fluidic channels to induce forces arising from fluidic flow to separate cells. Inertial devices are easy to use and require almost no additional supporting equipment. Aside from the microfluidic device, only a small portable syringe pump is required to inject cell-containing fluids at a consistent flow rate into the device. Canonical spiral inertial microfluidic designs use narrow channels (diameter < 150 μm) to separate cells into distinct focused streams [13,17–22]. Narrower channels generate larger forces to part cells into streams with larger separation distances. However narrow channels are not robust; inertial forces cannot separate all blood cells if there are a broad variety of cell sizes and narrow channels are prone to clogging. Furthermore, a slight manufacturing imprecision in the channel width relative to the intended design dimension will affect device performance (for example, a manufacturing variability of ±10μm in a 100μm width channel leads to significant deviation from intended performance). For this reason, inertial devices have been manufactured with high-precision lithographic manufacturing [23] and require stringent quality control. This fabrication method requires significant investment in infrastructure and skilled operators which can only be amortized by selling large quantities of the same device. It is prohibitive for resource-limited populations because the barriers to entry are too high.

We present our innovations to spiral inertial microfluidic device design that effectively separates blood cells sized between 6 μm to 15 μm into 3 separate streams. Our novel design utilizes larger channel sizes (200 μm to 600 μm) and is fabricated with the low-cost xurography [24,25] method, where a mask is cut from a polymer sheet. Using fluorescence beads, we validate that our device selects particles by size and subsequently validate the selection of white blood cells and dendritic cells as well as cell viability using flow cytometric analysis.

2. Materials and Methods

2.1 Device fabrication in resource-limited settings

The spiral microchannel was fabricated using a low-cost technique, xurography. The desired pattern was designed with a CAD software (AutoCAD version X, Autodesk Inc, CA, USA), and the pattern was cut into an adhesive vinyl sheet. The desired microchannel are removed from the sheet and filled

with epoxy polymer. The epoxy polymer was cured for 20 hours and inverse pattern of the microchannel is obtained in epoxy which will be used as a mold. The epoxy mold is used to manufacture polydimethylsiloxane (PDMS) spiral devices by replica molding. A mixture of PDMS base (pls insert) and curing agent (10:1 ratio) (pls insert) is cast on epoxy master and cured for 24 hours at room temperature. Cured PDMS devices embedded with channels are peeled off from the master mold, and inlet/outlet ports were punched using 2mm biopsy punch. The PDMS device is cleaned with scotch tape and ethanol. Subsequently, the device is permanently bonded to a standard glass slide using UV ozone system (Nova scan Inc., Iowa, US) for 5 minutes. The UV treated device is immediately baked in a hot plate at 80^{o}C for 15 minutes to increase the bonding strength.

2.2 Device validation with assay of polystyrene microparticles

Suspended 15µm diameter green fluorescent, 10µm non-fluorescent and 7µm diameter red fluorescent polystyrene microspheres (Bangs Laboratories) were mixed and diluted in deionized water with ~500,000 particles/ml. The mixture was then introduced into spiral microchannel using a programmable syringe pump (New Era NE-1000, New Era Pump Systems, Inc,) connected to the microchannel inlet with silicone tubing. Focused particle streams were visualized with an inverted microscope (Nikon Ti-S Microscope, CFI Plan Fluor 4X objective). Fluorescence and brightfield microscope images were captured with a 12-bit CCD Camera (Retiga Exi, QImaging).

2.3 Blood cells sample preparation

Blood samples were collected after informed consent and with approval by the Ethics Committee, Faculty of Dentistry, University of Malaya, DF OS0910/0049 (L). Freshly isolated PBMCs from the blood samples are cultured in M-SFM media and incubated for 1 hour at 37°C. Then the plates are shaken to loosen all non-attached cells and these were aspirated and removed. The adherent cells remaining on the plate were then cultured with M-SFM in the presence of 100ng/ml GM-CSF and 25ng/ml IL-4 to induce differentiation of dendritic cells. The cells were incubated in culture media for 5 days to grow and differentiate into mature dendritic cells. Mature DCs were centrifuged to remove the supernatant and final DC count obtained was ~35,000 cells / mL. 2 mL of DCs was mixed with 3 mL of diluted white and red blood cells (1000X dilution).

2.4 White blood cell and dendritic cell selection assay

The mixture of blood cells was injected into the device with a syringe pump at constant flow rate of 1.9mL/min and collected into 4 different outlets. Samples from each collection reservoir were stained with BD Horizon™ Fixable Viability Stain 780 (FVS780) viability dye (BD Biosciences Cat No. 565388) for 15 minutes at room temperature, followed by adding antibodies mixture comprised of Lineage cocktail 1 (BD Biosciences Cat No. 340546), PE conjugated mouse anti-human CD123 (BD Biosciences, Cat No 340545) and APC conjugated Mouse anti-human CD11c (BD Biosciences Cat No 340544) and further incubated for 30 minutes at 4°C. Following incubation, the cells were washed with phosphate buffer saline prior to flow cytometer analysis (BD FACSCanto II, BD Biosciences, New Jersey). The flow cytometer was used to quantify the purity and recovery rate of dendritic cells from our device. Viable dendritic cells are the sum of cells with CD11c+ and CD123- expression (typically myeloid DCs), cells with $CD123^{+}$ and $CD11c^{-}$ expression (typically plasmacytoid DCs) and cells expressing both markers.

$$\text{Recovery rate} = \frac{\text{number of WBCs in one outlet}}{\text{number of WBCs in all outlets}}$$

With the aid of a flow cytometer, we used FVS780 for discrimination of viable from non-viable mammalian cells. Blood cell mixture before and after processing by our spiral microfluidic device was mixed with FVS780 and quantified using BD FACS Canto II (BD Biosciences, USA).

$$\text{Viability rate} = \frac{\text{number of viable blood cells in each outlet}}{\text{total cell events in each outlet}}$$

2.5 Statistical analysis

Statistical analysis was conducted using GraphPad Prism 5. 1-way ANOVA was used compared the differences of viability and DC recovery from outlet 1-4. $p<0.05$ was considered as significant.

3. Results

3.1 Design and validation of novel inertial spiral device fluorescent bead separation assay

We developed a wallet-sized microfluidic device to separate human red, white blood and dendritic cells. Our device employs a spiral microfluidic channel with 7-turns, 100µm height and gradually increasing width from 200µm to 600µm (Figure 1a). Our device harnesses inertial forces arising from high velocity fluid flow in a curved channel to segregate blood cells in the fluid into focused streams by cell-size and into 4 collection outlets [19,26,27]. Using computational fluid dynamic simulations [26], we verified that our design would route particles of 15µm, 10µm and 7µm mean diameter into outlets 1, 2 and 3 respectively because we found that human dendritic cells are 10-15µm, white blood cells are 7-12µm and red blood cells are 6-8µm in size. Outlet 4 collects excess blood plasma. We tested a prototype device with a fluid mixture containing 15µm (green), 10µm (uncolored, white) and 7µm (red) fluorescent beads. Figure 1b illustrates the distribution of beads at various locations in our device during operation. The test validated that our device separates the 15µm, 10µm and 7µm beads into distinct streams narrowly spaced apart and routes the distinct particle streams into outlets 1, 2 and 3 respectively. Measurements reveal that 99% of the 15µm beads with 8% of 10µm and 1% of 7µm beads were routed into outlet 1. The remaining 92% of 10µm beads were routed into outlet 2 together with 8% of the 7µm beads [26].

3.2 Red, white blood and dendritic cell separation assay

Cells collected from all 4 outlets were assessed for their viability based on presence of white blood cell and dendritic cell surface markers using flow cytometry. More than 80% of cells passed through the four outlets remained viable; there is no significant difference in cell viability for cells passing through outlet 1, outlet 2, outlet 3 and outlet 4 (81.8%, 91.5%, 91.9% and 89.4% respectively) (Figure 2a & Table 1). Dendritic cells are concentrated in outlet 1 as an average of 77.2% DCs were collected from this outlet as compared to 15.1%, 6.5% and 1.2% (Figure 2b) from outlet 2,3 & 4 respectively ($p<0.0001$).

Table 1. The distribution of total and viable cells in all outlets show that cells remain equally viable across all outlets post enrichment

	Outlet 1				Outlet 2				Outlet 3				Outlet 4			
Trial	1	2	3	4	1	2	3	4	1	2	3	4	1	2	3	4
all cells count	221139	112753	213741	350905	57815	235055	97241	385416	34609	27504	120830	27327	20182	753	408	279
viable blood cells	165850	89809	193968	286347	48140	221070	92901	359696	29197	26026	115615	25372	18627	645	377	243
% of viable blood cells	75.0	79.7	90.7	81.6	83.3	94.1	95.5	93.3	84.4	94.6	95.7	92.8	92.3	85.7	92.4	87.1

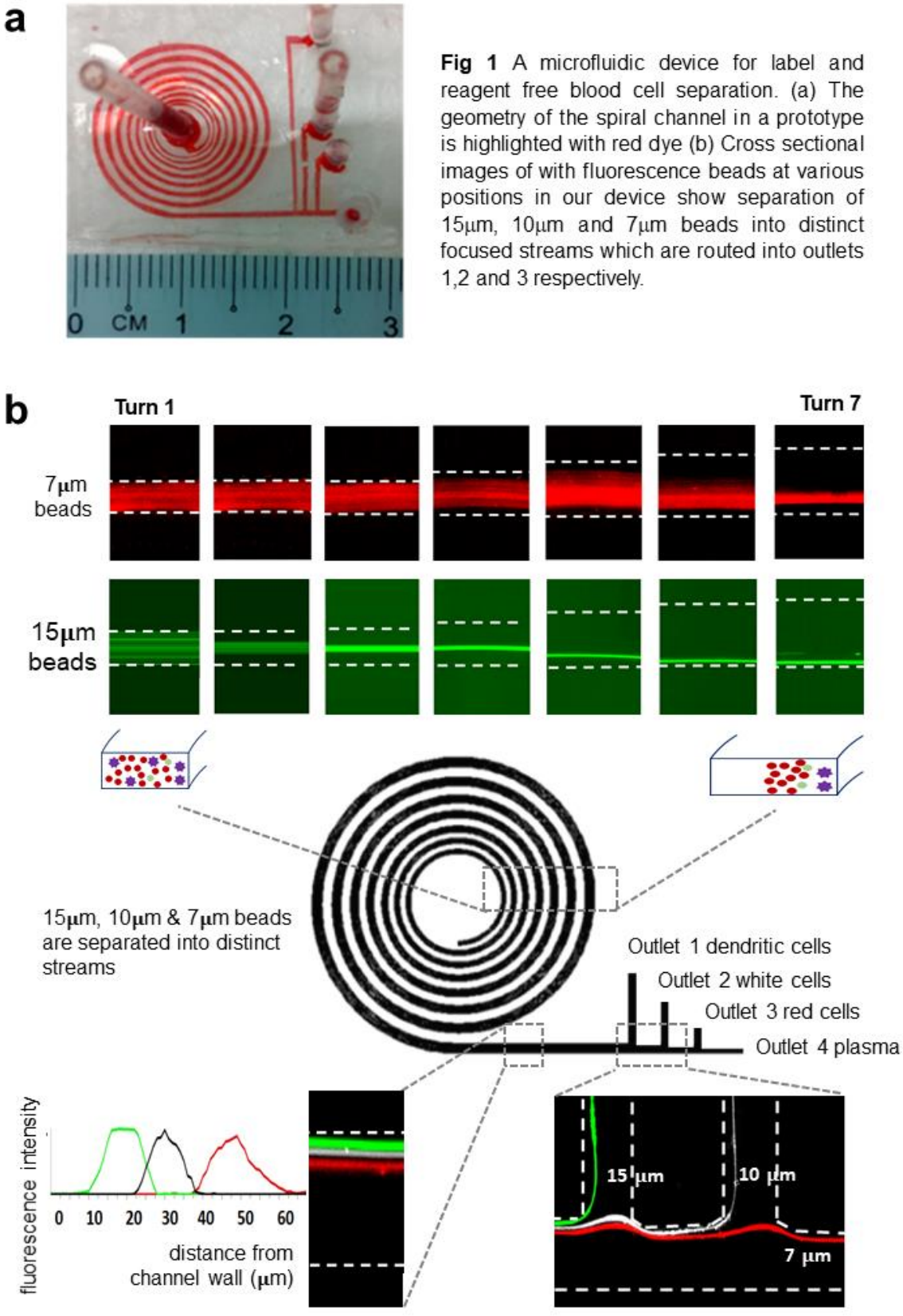

Fig 1 A microfluidic device for label and reagent free blood cell separation. (a) The geometry of the spiral channel in a prototype is highlighted with red dye (b) Cross sectional images of with fluorescence beads at various positions in our device show separation of 15μm, 10μm and 7μm beads into distinct focused streams which are routed into outlets 1,2 and 3 respectively.

Preprints (www.preprints.org) | NOT PEER-REVIEWED | Posted: 28 February 2020 doi:10.20944/preprints202002.0422.v1

Peer-reviewed version available at Micromachines 2020, 11, 514; doi:10.3390/mi11050514

Table 2. The distribution of dendritic cells and total blood cells in each outlet of the device show that dendritic cells are preferentially accumulated in Outlet 1 in an enriched population.

	Trial 1					Trial 2					Trial 3					Trial 4				
	Outlet 1	Outlet 2	Outlet 3	Outlet 4	All outlets	Outlet 1	Outlet 2	Outlet 3	Outlet 4	All outlets	Outlet 1	Outlet 2	Outlet 3	Outlet 4	All outlets	Outlet 1	Outlet 2	Outlet 3	Outlet 4	All outlets
all cells count	221139	57815	34609	20182	333745	112753	235055	27504	753	376065	213741	97241	120830	408	432220	350905	385416	27327	279	763927
dendritic cells	1080	125	108	47	1360	1818	419	47	16	2300	2667	406	561	20	3654	8922	2510	85	4	11521
% of total dendritic cells	79.4	9.2	7.9	3.5	100.0	79.0	18.2	2.0	0.7	100.0	73.0	11.1	15.4	0.5	100.0	77.4	21.8	0.7	0.0	100.0
dendritic cells as % of all cells	**0.5**	0.2	0.3	0.2	**0.4**	**1.6**	0.2	0.2	2.1	**0.6**	**1.2**	0.4	0.5	4.9	**0.8**	**2.5**	0.7	0.3	1.4	**1.5**

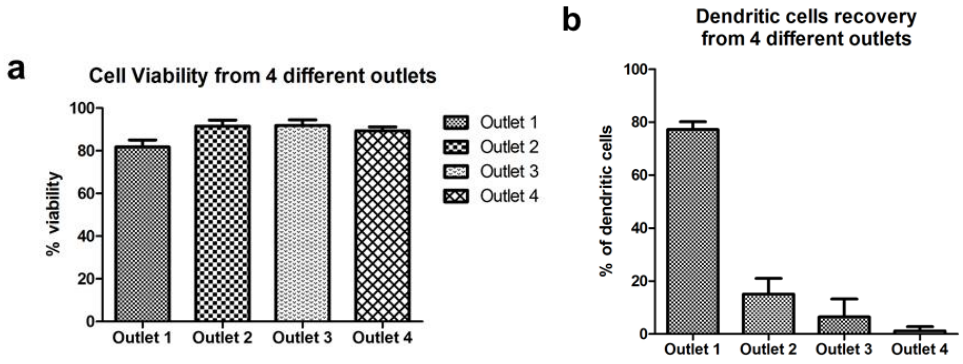

Figure 2. Distribution of viable dendritic cells in each collection outlet of our device (**a**) cells in each outlet are viable; (**b**) the majority of dendritic cells are collected in outlet 1.

4. Discussion

Spiral inertial devices induce inertial forces within a fluidic flow due to channel geometry, curvature (R_c) and high fluidic flow rates [28–30]. Two main forces act on cells (with size a_p) flowing with the fluid, lift force $\left(F_L \propto \frac{{a_p}^4}{wh}\right)$ (w: width and h: height)[34] and dean force $\left(F_D \propto \frac{a_p}{R_c}\right)$ [28], such that the balance between these forces migrate the cells to stable flow positions in focused and distinct streamlines. The ideal condition for cell separation is when the dean drag is on the same order as the inertial lift $(F_L \geq F_D)$, such that cells of different sizes experience different equilibrium forces and occupies size-dependent displacement across the channel cross-section. The lift force focuses cells while dean force separates cells into distinct streams. Two limiting cases should be avoided (1) $F_L \gg F_D$, cell migration is dominated solely by inertial lift and cells of all sizes are focused to the same equilibrium position; (2) $F_L \ll F_D$, the dominant dean force mixes cells through cross sectional channel flow and no focusing occurs.

Archetypical implementations of spiral separation devices use small channel widths relative to cell size to generate sufficient inertial lift force for focusing, because lift force is inversely proportional to channel dimensions $\left(F_L \propto \frac{{a_p}^4}{wh}\right)$. The magnitude of the inertial forces may be designed to be significantly larger than necessary to create sufficient gap between focused cells streams since the equilibrium position of cells of different sizes is dependent on the ratio of the inertial lift to dean force, ${F_L}/{F_D} = \left({a_p}/{h}\right)^3$ [18,29]. Most spiral designs have therefore been implemented with channel widths around 150 μm, which require precision fabrication techniques and economies of scale for cost efficiency.

However, narrow channel widths impose problems downstream when attempting to collect separated cells streams. When cells from a broad range of sizes must be separated, it becomes challenging to maintain the lift force to dean force ratio for cells of all sizes, if small channel widths are used, as some cells will inevitably become defocused and mix into other focused streams. There are insufficient degrees of freedom in the geometrical design parameters to enhance separation distance between multiple cell streams if small channel widths are used. Narrow width spiral devices cannot be fabricated without high precision lithographic techniques [31] which require significant infrastructure that cannot be easily set up in resource-limited settings. In the small channel width regime, only small variations in channel width dimensions can be tolerated, else the fabricated device will rapidly lose efficiency and not perform as intended [19,32].

Conventionally, the channel at the device outlet is divided into multiple outlets of narrower widths, to collect the focused cell streamlines into different outlets [18,19]. If many cell streams must be collected or if there is a small size difference between cells streams, the separation distance between two distinct cell streamlines can be very closely spaced (< 50 μm) [18] due to channel width constraints and become difficult to collect separately. Larger cells may clog the narrow outlets or become damaged from impact against the outlet walls. Expanding outlets have been designed to ameliorate the problem, but this causes the cells to defocus and mix.

Our design overcomes all these challenges and we demonstrate separation of multiple cell types (red blood cells, white blood cells, dendritic cells) without reagents or labels for true point-of-care operation. Our main innovation is in making spiral inertial designs work with larger-than-conventional channel widths. Although this runs against the prevailing trend in the microfluidics community towards miniaturization, using channel widths greater than 200 μm confers several distinct advantages. To our knowledge, ours is the first demonstration of how to sustain more than 2 separated focused streams of cells in spiral inertial devices. With larger channel widths, we are able to balance the inertial forces so that inertial focusing and separation effects apply to cells between 7 to 15 μm in size. Our design allows closely spaced cell streamlines (<50 μm) and does not need to generate large differential forces on differently sized cells because we have developed a novel design of large width collection channels [26] based on control of fluidic resistance without compromising collection efficiency. Channels exceeding 200 μm width can also be fabricated with less precise manufacturing methods, like xurography and are more tolerant to manufacturing variations. Our device is portable, simple to operate as it only requires a small syringe pump and can be fabricated and deployed in low resource settings. Only careful design of the channel geometry and operation at high fluid flow rates ~1.9 mL/min suffices. High throughput operation is an automatic feature because high flow rates into the device are necessary to initiate inertial forces for proper device operation. White blood cells and dendritic cells remained viable after enrichment. Since the majority (77.2%) of circulating dendritic cells are routed into outlet 1, simple size-based separation successfully separates dendritic cells from blood, and a significant portion of the white blood cells.

Our experiments with fluorescent beads confirm the size-selective function of our microfluidic device. However, large counts of both red and white mononuclear blood cells are also routed into outlet 1 and cells were also routed to outlet 4, which is not an intended feature of our design. A likely cause is the deterioration of inertial focusing effect due to dense blood cell concentrations. At cell-to-volume fractions between 1-3%, inertial forces are known to align cells laterally into a single stream and regulate interstream spacing [29,33]. Above that fraction, inertial focusing deteriorates presumably due to interparticle interactions [27]. We anticipate significant improvements in performance if we sufficiently dilute blood samples to achieve the preferred interstream spacing between cells which was derived from recent experimental studies [34,35].

Acknowledgments: ETWH thanks the Ministry of Education Malaysia for funding support through a grant awarded under the Fundamental Research Grant Scheme, which include the costs to publish in open access. CMY acknowledges Universiti Teknologi PETRONAS for graduate student assistantship.

Author Contributions: CMY and KPL contributed equally to this work. ETWH and SCC conceived the project. ETWH and NHH obtained funding for the project. CMY and IHK built the device. CMY and KPL performed the experiments and analysed the results. All authors wrote the paper.

Conflicts of Interest: The authors declare no conflict of interest. The funders had no role in the design of the study, in the collection, analyses, or interpretation of data, in the writing of the manuscript, and in the decision to publish the results.

References

1. Convery, N.; Gadegaard, N. 30 years of microfluidics. *Micro Nano Eng.* **2019**, *2*, 76–91.
2. Whitesides, G.M. The origins and the future of microfluidics. *Nature* **2006**, *442*, 368–373.
3. Littman, D.R. Releasing the Brakes on Cancer Immunotherapy. *Cell* **2015**, *162*, 1186–1190.

4. Drain, P.K.; Hyle, E.P.; Noubary, F.; Freedberg, K.A.; Wilson, D.; Bishai, W.R.; Rodriguez, W.; Bassett, I. V Diagnostic point-of-care tests in resource-limited settings. *Lancet. Infect. Dis.* **2014**, *14*, 239–249.
5. Chin, C.D.; Linder, V.; Sia, S.K. Commercialization of microfluidic point-of-care diagnostic devices. *Lab Chip* **2012**, *12*, 2118–2134.
6. Yousuff, C.; Ho, E.; Hussain K., I.; Hamid, N. Microfluidic Platform for Cell Isolation and Manipulation Based on Cell Properties. *Micromachines* **2017**, *8*, 15.
7. Ma, J.; Yan, S.; Miao, C.; Li, L.; Shi, W.; Liu, X.; Luo, Y.; Liu, T.; Lin, B.; Wu, W.; et al. Paper Microfluidics for Cell Analysis. *Adv. Healthc. Mater.* **2019**, *8*, 1801084.
8. Carrell, C.; Kava, A.; Nguyen, M.; Menger, R.; Munshi, Z.; Call, Z.; Nussbaum, M.; Henry, C. Beyond the lateral flow assay: A review of paper-based microfluidics. *Microelectron. Eng.* **2019**, *206*, 45–54.
9. Martinez, A.W.; Phillips, S.T.; Whitesides, G.M.; Carrilho, E. Diagnostics for the Developing World: Microfluidic Paper-Based Analytical Devices. *Anal. Chem.* **2010**, *82*, 3–10.
10. Palucka, K.; Banchereau, J. Cancer immunotherapy via dendritic cells. *Nat Rev Cancer* **2012**, *12*.
11. Gelao, L.; Criscitiello, C.; Esposito, A.; Laurentiis, M. De; Fumagalli, L.; Locatelli, M.A.; Minchella, I.; Santangelo, M.; Placido, S. De; Goldhirsch, A.; et al. Dendritic cell-based vaccines: clinical applications in breast cancer. *Immunotherapy* **2014**, *6*, 349–360.
12. Bol, K.F.; Schreibelt, G.; Gerritsen, W.R.; de Vries, I.J.M.; Figdor, C.G. Dendritic Cell-Based Immunotherapy: State of the Art and Beyond. *Clin. Cancer Res.* **2016**, *22*, 1897–1906.
13. Son, J.; Murphy, K.; Samuel, R.; Gale, B.K.; Carrell, D.T.; Hotaling, J.M. Non-motile sperm cell separation using a spiral channel. *Anal. Methods* **2015**, *7*, 8041–8047.
14. Lee, W.C.; Bhagat, A.A.S.; Huang, S.; Van Vliet, K.J.; Han, J.; Lim, C.T. High-throughput cell cycle synchronization using inertial forces in spiral microchannels. *Lab Chip* **2011**, *11*, 1359–1367.
15. Nathamgari, S.S.P.; Dong, B.; Zhou, F.; Kang, W.; Giraldo-Vela, J.P.; McGuire, T.; McNaughton, R.L.; Sun, C.; Kessler, J.A.; Espinosa, H.D. Isolating single cells in a neurosphere assay using inertial microfluidics. *Lab Chip* **2015**, *15*, 4591–4597.
16. Warkiani, M.E.; Tay, A.K.P.; Guan, G.; Han, J. Membrane-less microfiltration using inertial microfluidics. *Sci. Rep.* **2015**, *5*, 11018.
17. Sun, J.; Li, M.; Liu, C.; Zhang, Y.; Liu, D.; Liu, W.; Hu, G.; Jiang, X. Double spiral microchannel for label-free tumor cell separation and enrichment. *Lab Chip* **2012**, *12*, 3952–3960.
18. Nathamgari, S.S.P.; Dong, B.; Zhou, F.; Kang, W.; Giraldo-vela, J.P. Isolating single cells in a neurosphere assay using inertial microfluidics. *Lab Chip* **2015**, 4591–4597.
19. Kuntaegowdanahalli, S.S.; Bhagat, A.A.S.; Kumar, G.; Papautsky, I. Inertial microfluidics for continuous particle separation in spiral microchannels. *Lab Chip* **2009**, *9*, 2973–2980.
20. Khoo, B.L.; Warkiani, M.E.; Tan, D.S.W.; Bhagat, A.A.S.; Irwin, D.; Lau, D.P.; Lim, A.S.T.; Lim, K.H.; Krisna, S.S.; Lim, W.T.; et al. Clinical validation of an ultra high-throughput spiral microfluidics for the detection and enrichment of viable circulating tumor cells. *PLoS One* **2014**, *9*, 1–7.
21. Guan, G.; Wu, L.; Bhagat, A.A.; Li, Z.; Chen, P.C.Y.; Chao, S.; Ong, C.J.; Han, J. Spiral microchannel with rectangular and trapezoidal cross-sections for size based particle separation. *Sci. Rep.* **2013**, *3*, 1–9.
22. Nivedita, N.; Papautsky, I. Continuous separation of blood cells in spiral microfluidic devices. *Biomicrofluidics* **2013**, *7*, 054101.
23. Pinto, E.; Faustino, V.; Rodrigues, R.O.; Pinho, D.; Garcia, V.; Miranda, J.M.; Lima, R. A Rapid and Low-Cost Nonlithographic Method to Fabricate Biomedical Microdevices for Blood. *Micromachinesi* **2015**, *6*, 121–135.
24. Bartholomeusz, D.A.; Boutte, R.W.; Andrade, J.D. Xurography: rapid prototyping of microstructures

using a cutting plotter. *J. Microelectromechanical Syst.* **2005**, *14*, 1364–1374.

25. Speller, N.C.; Morbioli, G.G.; Cato, M.E.; Cantrell, T.P.; Leydon, E.M.; Schmidt, B.E.; Stockton, A.M. Cutting edge microfluidics: Xurography and a microwave. *Sensors Actuators B Chem.* **2019**, *291*, 250–256.
26. Mohamed Yousuff, C.; B Hamid, N.H.; Kamal Basha, I.H.; Wei Ho, E.T. Output channel design for collecting closely-spaced particle streams from spiral inertial separation devices. *AIP Adv.* **2017**, *7*, 085004.
27. Martel, J.M.; Toner, M. Inertial focusing dynamics in spiral microchannels. *Phys. Fluids* **2012**, *24*, 032001.
28. Bhagat, A.A.S.; Kuntaegowdanahalli, S.S.; Papautsky, I. Continuous particle separation in spiral microchannels using dean flows and differential migration. *Lab Chip* **2008**, *8*, 1906–1914.
29. Di Carlo, D.; Irimia, D.; Tompkins, R.G.; Toner, M. Continuous inertial focusing, ordering, and separation of particles in microchannels. *Proc. Natl. Acad. Sci.* **2007**, *104*, 18892–18897.
30. Di Carlo, D.; Edd, J.F.; Humphry, K.J.; Stone, H.A.; Toner, M. Particle segregation and dynamics in confined flows. *Phys. Rev. Lett.* **2009**, *102*, 94503.
31. Duffy, D.C.; McDonald, J.C.; Schueller, O.J.A.; Whitesides, G.M. Rapid Prototyping of Microfluidic Systems in Poly(dimethylsiloxane). *Anal. Chem.* **1998**, *70*, 4974–4984.
32. Zhang, J.; Li, W.; Li, M.; Alici, G.; Nguyen, N.-T. Particle inertial focusing and its mechanism in a serpentine microchannel. *Microfluid. Nanofluidics* **2014**, *17*, 305–316.
33. Lee, W.; Amini, H.; Stone, H.A.; Di Carlo, D. Dynamic self-assembly and control of microfluidic particle crystals. *Proc. Natl. Acad. Sci.* **2010**, *107*, 22413–22418.
34. Kahkeshani, S.; Haddadi, H.; Di Carlo, D. Preferred interparticle spacings in trains of particles in inertial microchannel flows. *J. Fluid Mech.* **2016**, *786*, R3.
35. Reece, A.E.; Oakey, J. Long-range forces affecting equilibrium inertial focusing behavior in straight high aspect ratio microfluidic channels. *Phys. Fluids* **2016**, *28*, 043303.